Jiroft refractory manganese ore leaching using oxalic acid as reducing agent in sulfuric acid solution

Arash Sobouti [1], Niosha Shafaat [2], Ali A. Abdollahzadeh [1,2]

[1] Department of Mining and Metallurgical Engineering, Amirkabir University of Technology, Tehran, Iran

[2] Department of Mining Engineering, University of Kashan, Iran

Corresponding author: abdzad@kashanu.ac.ir (A. Sobouti)

Abstract: Leaching process of Jiroft refractory manganese ore was investigated. The effects of operating parameters such as liquid to solid ratio, pulp temperature, sulfuric acid concentration, and oxalic acid concentration were studied and the optimization was done through the response surface methodology (RSM) based on central composite design (CCD) model. The recoveries of Mn, Fe and Si were selected as response of design. The optimum condition was determined by ANOVA, indicating that the liquid to solid ratio, oxalic acid concentration and pulp temperature for Mn recovery and liquid to solid ratio, pulp temperature and sulfuric acid concentration for Fe recovery and liquid to solid ratio for Si recovery were the most effective parameters, respectively. Under the optimum conditions of liquid to solid ratio= 11.8%, pulp temperature= 70 $^{\circ}$C, sulfuric acid concentration= 40 g/L and oxalic acid concentration= 35 g/L, 71.1%, 4.67% and 0.6% of Mn, Fe and Si were recovered, respectively.

1. Introduction

Manganese as the 10th most abundant element in the Earth's crust (about 0.1 percent of the crust), has uses in steel production, non-ferrous alloys, batteries, chemical industry and dietary additives (Zhang et al., 2018a, El Hazek et al., 2006).

Pure manganese has not been formed in nature and is mostly found in oxide, carbonate and silicate forms. The most important economic minerals of manganese are pyrolusite (MnO_2), hausmannite (Mn_3O_4), manganite ($MnOOH$), rhodochrosite ($MnCO_3$) and rhodonite ($MnSiO_3$), which are mostly found in metamorphic rocks or sedimentary deposits (Mehdilo et al., 2013, Zhang and Cheng, 2007, Hariprasad et al., 2018).

Pyrolusite could not react with sulfuric acid. A reducing agent convert the insoluble MnO_2 to soluble MnO. Manganese oxide ore can be extracted either by reduction–roasting followed by leaching or directly by reductive acid leaching using various reducing agents (Wang et al., 2017, Hariprasad et al., 2007, Zhang et al., 2018b, Habashi, 1993) such as ferrous sulfate (Vu et al., 2005), cornstalk (Cheng et al., 2009), sulfur dioxide (Sun et al., 2013), hydrogen peroxide (Khan and Kurny, 2014), sodium sulfide (Sheng and QIU, 2014), carbohydrates (Wu et al., 2014), waste tea (Qing et al., 2014), ethylenediaminetetraacetic acid (EDTA) (Zhang et al., 2018a, Zhang et al., 2018b), glucose(Pagnanelli et al., 2004), sawdust (Hariprasad et al., 2007) and oxalic acid(Sahoo et al., 2001).

The main problems with these hydrometallurgical processes are the purification of Mn from the leaching solution, high production cost and low leaching efficiency (Gadd, 1999).

Oxalic acid is a weak and organic acid, eco-friendly and usually used as a leaching agent (Kusumaningrum et al., 2019).

The reaction of MnO_2 in the low manganese ore with oxalic acid in sulfuric acid solution could occur as follows (Abbruzzese et al., 1990):

$$MnO_2 + C_2H_2O_4 + H_2SO_4 \rightarrow Mn^{2+} + 2CO_2 + 2H_2O \tag{1}$$
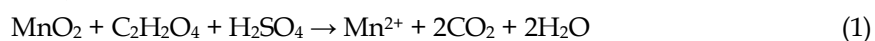
The proposed dissolution mechanism occurs through the adsorption of oxalate ion onto the oxide surface layers, followed by the reduction reaction via electron transfer (Godunov et al., 2012).

Sahoo et al. (2001) studied the leaching of low-grade manganese ore using oxalic acid as reductant in sulphuric acid solution. The results showed that the recovery of manganese was 98.4% in the conditions of 30.6 g/l oxalic acid, 0.543 mol/L sulfuric acid after 105 minutes of leaching at pulp temperature of 85 °C (Sahoo et al., 2001).

Azizi et al. (2012) studied the leaching of low-grade manganese bearing ore. They showed that oxalic acid and sulfuric acid concentration has significant effect on the recovery of manganese. Also, they showed that pulp temperature and leaching time has less effect on the recovery of manganese (Azizi et al., 2012).

RSM is a statistical and scientific method used for multiplex return investigation utilizing quantitative information extracted from appropriately designed experiments to explain multivariable equations at the same time. It is a helpful method for designing experiments, model structure, assessing the impacts of experimental parameters and deciding ideal conditions for alluring responses. The central composite design (CCD), one of the systems in RSM, is utilized broadly to structure the second order response surface models (Dong et al., 2010).

In this study, the leaching of Jiroft manganese ore using oxalic acid as a reductant in sulfuric acid solution was comprehensively evaluated based on the optimization process. In this regard, the effects of important factors such as oxalic acid concentration, pulp temperature, sulfuric acid concentration and liquid to solid were evaluated using the response surface methodology (RSM) based on central composite design (CCD) model.

2.   Materials and methods

2.1. Data set

The ore samples were obtained from Jiroft Mahmoud Abad mine, in Kerman province, Iran. The samples were crushed and ground by laboratory jaw crusher and ball mill to less than 1mm and then screened to 80% passing through 0.74 mm in advance. Table 1 shows the size distribution analysis of Mn, Fe and Si. The results show that 56.3% of the feed is below 300 micron which is an appropriate size for leaching. Also, different fractions of the samples were also analyzed to calculate Mn, Fe and Si distribution in specified sections. According to the results in Table 1, Mn grade has a homogenous distribution in different size fractions. Therefore, a feed with particle size of below 300 microns were used for leaching tests.

In order to determine the mineralogical composition of sample, XRD analysis using X'Pert MPD Philips, Holland) was carried out (Fig. 1). As characterized by XRD, the main minerals are hematite (Fe_2O_3), quartz (SiO_2) and calcite ($CaCO_3$). However, manganese minerals were not detected in the sample despite the chemical analysis results. This could be due to the lack of complete crystallization or masking of manganese mineral phases. This distribution shows the sensitivity of the ore to enrichment. In the mineralogy studies, the thin and polished sections were examined by ZEISS Polarized Optical Microscope (Axioplan 2). The minerals manganite, hematite and quartz are more than 10%, calcite and pyrolusite minerals are less than 10%, forming the trace minerals of the sample. Manganite is in the form of small veins in the sample. Also, for the degree of liberation studies, fractional samples of polished sections were prepared and examined. As results, the grains contain of manganite-hematite-calcite-quartz, as well as manganite-hematite-calcite and manganite-hematite-quartz have been reported.

Manganese minerals in the fraction (-75+53) microns are about 80% liberated. Most of the gangue minerals, calcite and quartz, in the sample are locked with the manganese and iron minerals to a degree and also as inclusion are in manganese and iron minerals. Chemical analysis of the samples performed by X-ray fluorescence (XRF) (Philips X Unique II). Analysis showed that content of Mn, Fe and SiO_2, is 20.47%, 13.5% and 32.07% respectively (Table 2).

The scanning electron microscope (SEM) and energy dispersive spectroscopy (EDS) images of the ore sample obtained by Philip XL30 scanning electron microscope are presented in Fig. 2. The morphology and the main constituent of the mineral are shown in Fig. 2. In this figure, some of the manganese is in form of manganese-silica compound and the other is manganite. The EDX analysis

result and the chemical analysis results are consistent. SEM and EDX analysis showed that the main contents were Mn, Fe, O and Si.

Table 1. Size distribution analysis of Mn, Fe and Si

Particle size (micron)	Weight (%)	Cumulative retained (%)	Cumulative passing (%)	Grade Mn (%)	Grade Fe (%)	Grade Si (%)	Distribution Mn (%)	Distribution Fe (%)	Distribution Si (%)
-1000+500	38.6	38.6	61.4	21.12	19.77	32.00	40.57	38.12	38.67
-500+300	17.7	56.3	43.7	20.3	19.17	30.89	17.9	16.97	17.14
-300+150	19.8	76.1	23.9	20.34	20.29	31.57	20.11	20.15	19.64
-150+75	9.5	85.6	14.4	19.85	19.55	31.77	9.39	9.29	9.46
-75+53	2.5	88.2	11.8	19.68	20.64	31.52	2.48	2.61	2.5
-53+38	2.7	90.8	9.2	19.41	22.52	29.65	2.58	3	2.48
-38	9.2	100.00	---	15.29	21.51	35.19	6.98	9.86	10.11
Total	100	---	---	20.09	20	31.91	100	100	100

Table 2. XRF of the sample (mass fraction %)

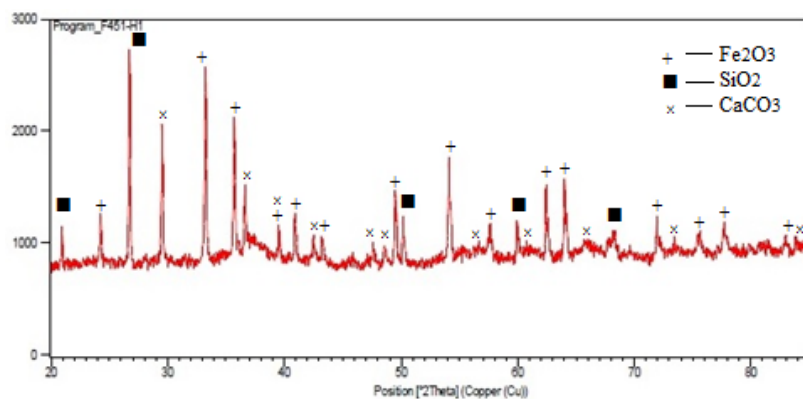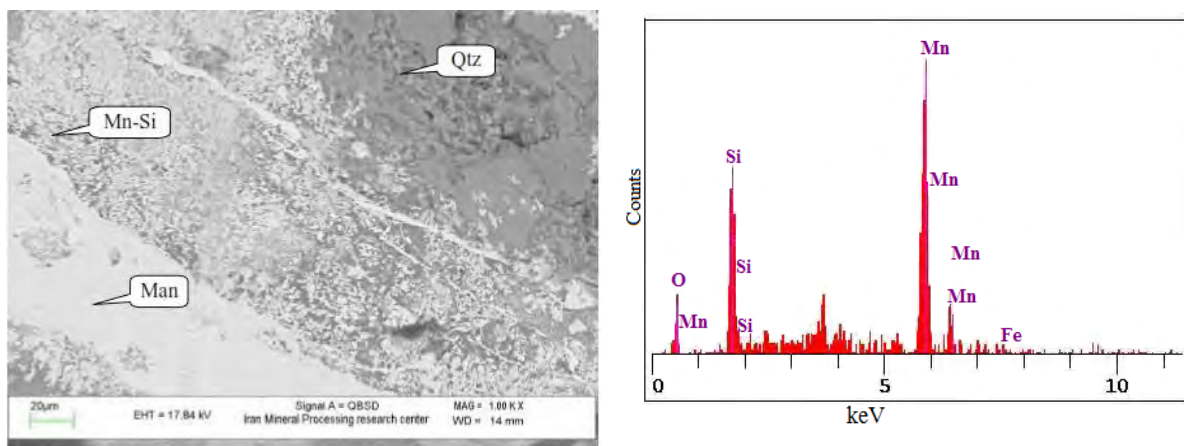| MgO	Al$_2$O$_3$	SiO$_2$	P$_2$O$_5$	MnO	Fe$_2$O$_3$	K$_2$O	CaO	TiO$_2$
0.855	2.13	32.07	0.14	26.43	19.66	0.135	3.7	0.145

Fig. 1. XRD pattern of sample before leaching

Fig. 2. SEM/EDS data of sample

2.2. Chemical reactions and equipment

Sulfuric acid (H$_2$SO$_4$) (96–98%, Merck) and Oxalic acid (C$_2$H$_2$O$_4$) were were used as lixiviant and reducing agent in the leaching experiments, respectively. Leaching experiments were conducted in a

beaker of 1000 ml which heated by hot plate, equipped with a digital controlled magnetic stirrer and a thermometer for temperature control. A typical experiment was conducted as follows: A series of sulfuric acid and oxalic acid with various concentrations was prepared as the leaching agent and put into the beaker. The target temperature was set. In order to prepare a pulp with desired solid percentage, 20 g of sample and required amount of distilled water were added into the beaker. Then, the slurry was mixed using a magnetic stirrer with a 550 rpm of speed at the required temperature. When the leaching process finished according to required time interval, the slurry was filtered and the residue was washed with distilled water and the liquid phase was analyzed.

Manganese concentration was determined by using the Atomic Absorption Spectrometry (AAS) (Perkin Elmer AA300 model). The percentage of dissolution was calculated from the following equation:

$$R= (C_1 \times V) / (C_0 \times M) \tag{2}$$

where R is the recovery; C_1 (g/l) is the concentration of manganese ion in the leach liquor; V (l) is the leach liquor volume; C_0 (%) is the metal content of manganese in the sample and M (g) is the weight of sample used in the experiment.

2.3. DOE

Design of experiments (DOE) methodology has been widely used in the optimization of many processes. In addition to optimization, a significant benefit of the DOE approach is the ability to identify significant interactions between factors. Response surface methodology (RSM) is one of effective methods of DOE(Fegade et al., 2013, Sobouti et al., 2019).

The RSM is a useful method for optimization process when the response depends on some independent factors and their interactions. In the RSM method, an experimental design is designed to fit a model based on the minimum squares method. Then, the proposed model adequacy is evaluated using the analysis of variance (ANOVA). Central composite design (CCD) is one of the most commonly used methods in RSM. A CCD was used to determine the optimal conditions for the significant factors (Fegade et al., 2013, Deihimi et al., 2018, Sobouti et al., 2019).

In this work, the RSM based on a CCD was used for the experiment to study the operating parameters affecting on the recovery of manganese by Design expert 7 (DX7) statistical software. Based on the literature and elementary experiments, the parameters considered as experimental design input include liquid to solid (A), pulp temperature (B), oxalic acid concentration (C) and sulfuric acid concentration (D). The codes and variation levels of operating parameters are listed in Table 3. Through the central composite design method, 30 experiments were designed as shown in Table 4.

Table 3. Independent variables and their levels in central composite rotatable design

Variables	Symbol	Codes and levels				
		-2	-1	0	+1	+2
Solid percent/ (%)	A	5	10	15	20	25
Leaching temperature/(^oC)	B	25	40	55	70	85
Sulfuric acid concentration/(g/L)	C	25	40	55	70	85
Oxalic acid concentration/(g/L)	D	12.5	20	27.5	35	42.5

3.   Results and discussion

3.1. ANOVA analysis

The recovery of Mn, Fe and Si for the 30 leaching experiments is presented in Table 4. The analyis of variance ANOVA was carried out for these results to determine whether the effects of process factors are statistically significant and it was used to analyze and suggest a mathematical model based on experimental leaching recovery data(Hoseinian et al., 2019). The ANOVA analysis of Mn, Fe and Si extraction is shown in Table 5. The mean squares (MS) are obtained as: MS = SS/DF, where: SS = sum of squares (SS) of each variation source and DF = the respective degrees of freedom (Df) (Myers et al., 2016). A quadratic equation was derived to predict the Manganese recovery as a function of independent variables and their interactions in terms of coded factors. The quadratic equation is as fol-

Table 4. Experiments designed by CCD method and obtained results

Test No.	A	B	C	D	Mn recovery %		Fe recovery %		Si recovery %	
					Experimental	Predicted	Experimental	Predicted	Experimental	Predicted
1	-1	-1	-1	1	65.57	66.22	2.06	2.79	0.58	0.66
2	-1	1	-1	-1	74.2	62.3	8.91	7.87	0.56	0.56
3	0	2	0	0	53.4	58.57	4.9	6.31	0.39	0.39
4	1	1	-1	-1	32.42	29.33	2.35	2.09	0.3	0.29
5	0	0	0	0	47.25	40.66	5.68	4.63	0.62	0.55
6	0	-2	0	0	51.94	45.63	3.49	1.46	0.55	0.44
7	1	-1	1	1	26.42	38.18	2.14	4.03	0.27	0.33
8	0	0	2	0	54.05	49.09	9.17	8.52	0.33	0.24
9	0	0	0	0	34.06	40.66	4.3	4.63	0.59	0.55
10	1	1	1	-1	26.55	25.76	5.63	5.75	0.27	0.24
11	1	-1	1	-1	31.1	26.85	4.7	4.49	0.24	0.35
12	0	0	0	0	44.18	40.66	4.2	4.63	0.53	0.55
13	0	0	0	0	34.12	40.66	3.75	4.63	0.56	0.55
14	1	1	-1	1	39.87	40.34	0.48	0.37	0.19	0.27
15	0	0	0	2	72.25	64.51	4.42	4.04	0.54	0.49
16	-1	1	1	-1	60	64.01	12.98	12.99	0.37	0.47
17	-1	-1	1	1	61.5	65.87	6.87	6.9	0.64	0.71
18	0	0	0	0	39.04	40.66	5.2	4.63	0.5	0.55
19	1	1	1	1	53.46	47.2	7.34	5.88	0.27	0.31
20	-1	-1	1	-1	48.2	47.59	6.18	7.15	0.62	0.63
21	-1	1	1	1	89.57	92.4	12.76	13.33	0.77	0.73
22	-2	0	0	0	90.8	85.16	14.2	13.28	1.11	1.10
23	-1	1	-1	1	74.72	80.25	6.4	6.37	0.77	0.72
24	0	0	0	0	45.3	40.66	4.65	4.63	0.51	0.55
25	0	0	-2	0	49.2	53.02	0.71	0.74	0.26	0.24
26	2	0	0	0	20	24.5	4.32	4.62	0.53	0.43
27	0	0	0	-2	28.61	35.21	6.24	6.00	0.44	0.38
28	1	-1	-1	1	46.55	43.82	1.61	1.37	0.25	0.21
29	1	-1	-1	-1	45.88	42.91	3.39	3.67	0.27	0.36
30	-1	-1	-1	-1	50.83	58.37	3.66	4.88	0.62	0.58

lows:

- for Mn recovery:

$$y_1 = 40.66 - 15.16A + 7.32D - 4.38AB \tag{3}$$

- for Fe recovery:

$$y_2 = 4.63 - 2.16A + 1.21B + 1.94C - 1.15AB - 0.36AC + 0.71BC + 1.08A^2 \tag{4}$$

- for Si recovery:

$$y_3 = 0.55 - 0.17A + 0.053A^2 - 0.078C^2 \tag{5}$$

where A, B, C and D are coded values of the tests variables, A: liquid to solid, B: pulp temperature, C: sulfuric acid concentration and D: oxalic acid concentration.

Table 5 shows the variance analyses of regression variables of the Mn recovery, Fe recovery and Si recovery models, respectively. The F-value and p-value of the Mn recovery model were 9.83 and < 0.0001, it was 16.45 and < 0.0001 for the Fe recovery model, and it was 10.66 and < 0.0001 for the Si recovery model that indicated that the models were significant. The Prob > F values of model terms of less than 0.05 indicate that they are significant(Behera et al., 2018).

A, D, AB, and A^2 are significant factors in the Mn recovery model. A, B, C, AB, BC, and A^2 are significant factors in the Fe recovery model. A, A^2 and C^2 are significant factors in the Si recovery model.

The statistical measures and model performance of Mn recovery, Fe recovery and Si recovery are presented in Table 6. The model's adequate precision ratio is an adequate signal for the appropriate model that was 12.24 for the Mn recovery model and 15.683 for the Fe recovery model and 14.718 for the Si recovery model (adequate precision > 4). The R^2 values for Mn recovery, Fe recovery and Si recovery are 0.9017, 0.9389 and 0.9086, respectively, which indicates that the models are appropriate. The result showed that the efficiency of these models is appropriate for predicting the recovery of Mn, Fe and Si.

The model can estimate the test values with appropriate precision when the obtained residuals have a normal distribution. Fig. 3 shows the absolute values of residual differences between the test residuals and achieved response from the model.

Table 5. ANOVA analysis results of the developed model for (a) Mn recovery (b) Fe recovery (c) Si recovery

Source	SS	Df	MS	F-Value	p-value
(a)					
Model	8470.45	14	605.03	9.83	< 0.0001
A	5518.85	1	5518.85	89.68	< 0.0001
B	251.29	1	251.29	4.08	0.0615
C	23.09	1	23.09	0.38	0.5494
D	1287.15	1	1287.15	20.91	0.0004
AB	306.6	1	306.6	4.98	0.0413
AC	27.93	1	27.93	4.50E-01	0.5108
AD	48.23	1	48.23	0.78	0.39
BC	156.13	1	156.13	2.54	0.1321
BD	102.11	1	102.11	1.66	0.2172
CD	108.78	1	108.78	1.77	0.2035
A²	344.33	1	344.33	5.6	0.0319
B²	224.45	1	224.45	3.65	0.0755
C²	185.33	1	185.33	3.01	0.1032
D²	145.18	1	145.18	2.36	0.1454
Residual	923.13	15	61.54		
Lack of Fit	756.83	10	75.68	2.28	0.1885
Pure Error	166.3	5	33.26		
Cor Total	9393.59	29			
(b)					
Model	314.67	14	22.48	16.45	< 0.0001
A	112.41	1	112.41	82.28	< 0.0001
B	35.19	1	35.19	25.76	0.0001
C	90.71	1	90.71	66.4	< 0.0001
D	5.78	1	5.78	4.23	0.0575
AB	20.98	1	20.98	15.35	0.0014
AC	2.09	1	2.09	1.53	0.2354
AD	0.046	1	0.046	0.034	0.8565
BC	8.12	1	8.12	5.95	0.0277
BD	0.35	1	0.35	0.25	0.621
CD	3.4	1	3.4	2.49	0.1353
A²	31.99	1	31.99	23.42	0.0002
B²	0.95	1	0.95	0.7	0.4171
C²	0	1	0	0	1
D²	0.26	1	0.26	0.19	0.6684
Residual	20.49	15	1.37		
Lack of Fit	18	10	1.8	3.61	0.0848

|					*Continued*
Pure Error	2.5	5	0.5		
Cor Total	335.16	29			
(c)					
Model	1.09	14	0.078	10.66	< 0.0001
A	0.68	1	0.68	92.96	< 0.0001
B	4.00E-03	1	4.00E-03	0.55	0.4697
C	1.04E-04	1	1.04E-04	0.014	0.9064
D	0.02	1	0.02	2.73	0.1196
AB	6.25E-06	1	6.25E-06	8.59E-04	0.977
AC	1.81E-03	1	1.81E-03	0.25	0.6256
AD	0.03	1	0.03	4.09	0.0614
BC	2.26E-03	1	2.26E-03	0.31	0.5859
BD	0.016	1	0.016	2.23	0.1558
CD	0.011	1	0.011	1.44	0.2482
A^2	0.078	1	0.078	10.76	0.0051
B^2	0.032	1	0.032	4.37	0.054
C^2	0.17	1	0.17	22.81	0.0002
D^2	0.023	1	0.023	3.18	0.0947
Residual	0.11	15	7.28E-03		
Lack of Fit	0.098	10	9.81E-03	4.43	0.0572
Pure Error	0.011	5	2.22E-03		
Cor Total	1.2	29			
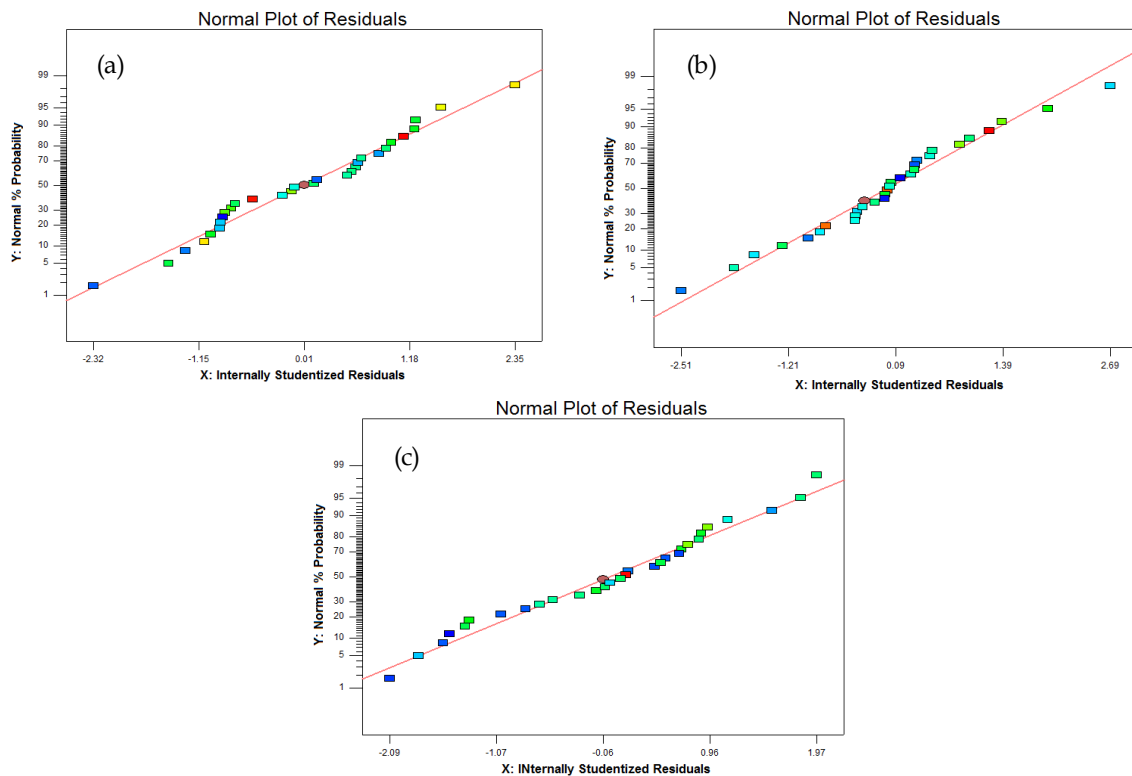
Fig. 3. Normal plot of residual for (a) Mn recovery (b) Fe recovery (c) Si recovery

As shown in Fig. 3(a), Fig. 3(b) and Fig. 3(c) the obtained results from the model have a good fit with the results of experiments. The lack of particular trends in residual values versus the test numbers

showed that there are not any systematic errors in performing the tests. Systematic errors led to an increase or decrease in the residual values.

3.2. Effect of parameters

Fig. 4 shows the comparative effects of solid percent, temperature, sulfuric acid concentration, and oxalic acid concentration on Mn, Fe recovery and Si recovery in the conditions of liquid to solid ratio (A) = 15%, pulp temperature (B) = 55 °C, sulfuric acid concentration (C) = 55 g/L, and oxalic acid concentration (D) = 27.5 g/L. The effect of parameters such as; solid percent, temperature, sulfuric and oxalic acids concentration on the Mn recovery were evaluated. As can be seen in Fig. 4(a), a sharp curvature in solid percent and oxalic acid concentration shows that the Mn recovery was very sensitive to these variables. The results showed that the solid percent has the most effect on the Mn recovery; actually, decrease of the solid percent increases the Mn recovery. The result is similar to the previous work by Zhang et al. (2013) and Hariprasad et al. (2007) that the leaching rate of the ore sample increased with the decreasing solid percent(Hariprasad et al., 2007, Zhang et al., 2013). Generally, the leaching rate increases with reducing the pulp density since high amount of leaching agent is added to a low content of solid(Habashi, 1993).

Table 6. Statistical measures and models performance of Mn, Fe and Si recovery

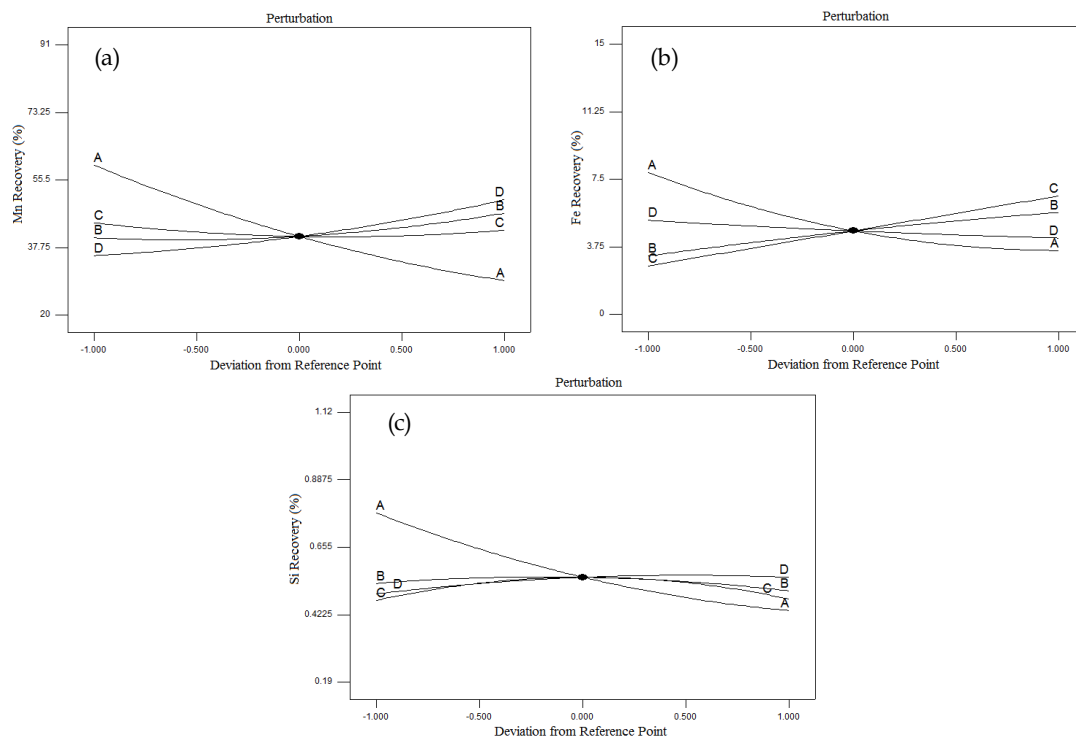| Model	R²	SD	Mean	Coefficient of variation (%)	Adequate precision
Mn recovery	0.9017	7.84	49.7	15.78	12.24
Fe recovery	0.9389	1.17	5.42	21.55	15.683
Si recovery	0.9086	0.085	0.48	17.71	14.718

Fig. 4. Perturbation plot for (a) Mn recovery (b) Fe recovery and (c) Si recovery (actual factor: A = 15 %, B = 55 °C, C = 55 g, and D = 27.5 g)

Increasing oxalic acid concentration has increased the Mn recovery. The result can be explained on the fact that the manganese ores is insoluble in sulfuric acid solution in absence of a reducing agent, but in the presence of oxalic acid that used as reducing agent, Mn^{+4} is converted to Mn^{+2} which was easily leached in sulfuric acid solution according to Eqs. (1).

While other parameters have lower influence on the Mn recovery. The Mn recovery is increased with increasing the temperature because of the active molecular motion and also the reaction is endothermic. The sulfuric acid concentration curve shows less sensitivity of Mn recovery to changes in this variable.

As can be seen in Fig. 4(b), a sharp curvature in solid percent, temperature and sulfuric acid concentration shows that the Fe recovery was very sensitive to these variables.
The results showed that the solid percent has also the most effect on the Fe recovery, The Fe recovery increases with decreasing of solid percent. The Fe recovery increases with increasing the temperature and sulfuric acid concentration. The oxalic acid concentration has no significant effect on Fe recovery.

As can be seen in Fig. 4(c), only the solid percent has effect on the Si recovery, while the other parameters have no significant effect on Si recovery.

The three-dimensional plots of the model show the effect of interaction of process variables. In these plots, two variables changed in the experimental ranges while the other variable was constant. The 3D plots of Mn, Fe and Si recovery using DX7 software is shown in Figs. 5, 6 and 7, respectively.

Fig. 5 shows the mutual effect of solid percent and temperature on Mn recovery. When solid percent was increased, the amount of dissolved ore per unit liquid increase consequently the recovery decreases. This result is attributed to the fact that the decrease in the solid percent not only decreases the suspension density, but also reduces the viscosity of the system and therefore decreases the mass transfer resistance at the liquid–solid interface. As can be seen, increasing the temperature enhances the recovery at all solid percent although the slope is higher at lower solid percent. Temperature increase enhances the rate of endothermic reaction. Temperature strongly influences the leaching rate of metals. Increasing the temperature cause to the decrease of solution viscosity and also increases the filtration rate.

Fig. 6 shows the mutual effect of solid percent and temperature on the Fe recovery. As can be seen, at lower of solid percent, the recovery is increased with increasing the temperature. In the higher amount of solid percent, the temperature has a weaker effect on the Fe recovery. Temperature had a significant effect on the Fe recovery. As a consequence, the temperature is one of the main parameters in the leaching process.
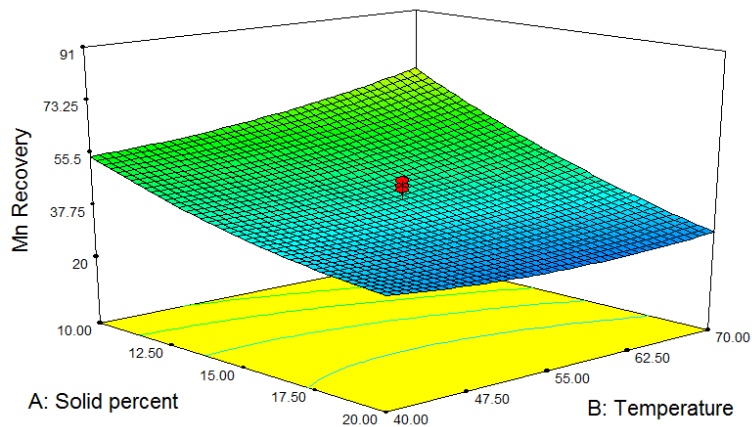

Fig. 5. Effect of solid percent and temperature on Mn recovery

Fig. 6. Effect of solid percent and temperature on Fe recovery

Fig. 7 shows the mutual effect of sulfuric acid concentration and temperature on Fe recovery. As can be seen, the Fe recovery is increased with increasing the sulfuric acid concentration and temperature. Because the dissolution rate perhaps was proportional to the concentration of the reducing species on the surface of the dissolving solid.

Fig. 7. Effect of sulfuric acid concentration and temperature on Fe recovery

3.3. Optimization

Finding an optimum condition of leaching process with the highest Mn recovery and the lowest consumption of reagents was the main object of this investigation. The response surface quadratic model was analyzed by design expert software. Variables can be minimum or maximum in this location; also, economics was considered to find a desirable location. In this research, the response surface methodology was used by DX7 software to find the best condition of manganese leaching process. The results of the process optimization and optimum levels of variables with various targets are displayed in Table 7. The first predicted conditions considered maximum level of Mn recovery and minimum levels of Fe and Si recoveries and maximum amounts of variables as the optimization target. The Mn,

Table 7. Results of process optimization and optimum levels of variables

No.	Case	Target	Solid percent/ %	Temp./ °C	Sulfuric acid Conc./ g.L^{-1}	Oxalic acid Conc. / g.L^{-1}	Mn recov./ %	Fe recov./ %	Si recov./ %	Desira-bility
	Mn recovery	Max								
1	Fe recovery	Min	15.1	70	70	35	65.72	8.43	0.47	0.681
	Si recovery	Min								

	Variables	Max								
	Mn recovery	Max								
	Fe recovery	Min								
2	Si recovery	Min	12	70	44.6	35	70.82	5.52	0.64	0.611
	Variables	In range								
	Mn recovery	Max								
	Fe recovery	Min								
	Si recovery	Min								
	Solid percent	In range								
3	Temp.		11.8	70	40	35	71.1	4.67	0.6	0.745
	Sulfuric acid Conc.	Min								
	Oxalic acid Conc.	Max								

Fe and Si recoveries reached 65.72%, 8.43% and 0.47%, respectively; also, sulfuric and oxalic acids concocentration were 70 g/L and 35 g/L and solid percent and temperature of the process were 15.1% and 70°C approximately, respectively. The desirability of this predicted condition achieved 0.681. The second predicted conditions considered maximum level of the Mn recovery and minimum levels of the Fe and Si recoveries and amounts of variables are in range. The Mn, Fe and Si recoveries reached 70.82%, 5.52% and 0.64%, respectively. Sulfuric and oxalic acid concentrations achieved 44.6 g/L and 35 g/L, and solid percent and temperature of the process were 12% and 70°C, respectively. The desirability of this condition was 0.611. Finally, the third predicted conditions considered maximum level of the Mn recovery and minimum levels of the Fe and Si recoveries and amounts of solid percent and temperature are in range and amount of sulfuric acid concentration is minimum and amount of and oxalic acid concentration is maximum. The Mn, Fe and Si recoveries reached 71.1%, 4.67% and 0.6%, respectively. The solid percent and temperature of the process were 11.8% and 70 °C, respectively. Sulfuric and oxalic acid concentrations achieved 40 g/L and 35 g/L, respectively. The desirability of this predicted condition achieved 0.745. The third predicted conditions show the best compared with the other conditions. Indeed, it was chosen as the best optimum condition by DX7 software. On the other hand, both the desirability of third prediction and Mn dissolution were higher while Fe and Si recoveries were the lowest.

4. Conclusions

The refractory manganese leaching was investigated using oxalic acid as an oxidant agent for Mn recovery. The RSM based on CCD principle was used for experimental design and optimization. The important variables such as solid percent, temperature, oxalic and sulfuric acid concentration and their interaction in Mn, Fe and Si recovery were evaluated. In optimum conditions, the Mn, Fe and Si recoveries of 71.1%, 4.67% and 0.6% were obtained, respectively; also, the desirability of optimum condition was approximately 0.745. The optimum conditions were: solid percent= 11.8%, temperature= 70°C, sulfuric acid concentration= 40 g/L and oxalic acid concentration= 35 g/L. The results indicate that the Mn, Fe and Si recoveries during the process were decreased with increasing the solid percent, while the oxalic acid concentration did not have a significant effect on Fe recovery. Oxalic acid concentration and temperature had significant positive effect on the Mn recovery. According to the result of Mn recovery, oxalic acid has greater leaching capacity due to its affinity to bind with Mn and act as the reducing agent by providing H^+ ion. Oxalic acid has high affinity toward Mn and form Mn-oxalate complexes which leach out manganese from the ore.

Acknowledgments

References

ABBRUZZESE, C., DUARTE, M., PAPONETTI, B. & TORO, L. 1990. *Biological and chemical processing of low-grade manganese ores.* Minerals Engineering, 3**,** 307-318.

AZIZI, D., SHAFAEI, S. Z., NOAPARAST, M. & ABDOLLAHI, H. 2012. *Modeling and optimization of low-grade Mn bearing ore leaching using response surface methodology and central composite rotatable design.* Transactions of Nonferrous Metals Society of China, 22, 2295-2305.

BEHERA, S. K., MEENA, H., CHAKRABORTY, S. & MEIKAP, B. 2018. *Application of response surface methodology (RSM) for optimization of leaching parameters for ash reduction from low-grade coal.* International Journal of Mining Science and Technology, 28**,** 621-629.

CHENG, Z., ZHU, G. & ZHAO, Y. 2009. *Study in reduction-roast leaching manganese from low-grade manganese dioxide ores using cornstalk as reductant.* Hydrometallurgy, 96**,** 176-179.

DEIHIMI, N., IRANNAJAD, M. & REZAI, B. 2018. *Equilibrium and kinetic studies of ferricyanide adsorption from aqueous solution by activated red mud.* Journal of environmental management, 227**,** 277-285.

DONG, L., PARK, K.-H., ZHAN, W. & GUO, X.-Y. 2010. *Response surface design for nickel recovery from laterite by sulfation-roasting-leaching process.* Transactions of Nonferrous Metals Society of China, 20**,** s92-s96.

EL HAZEK, M., LASHEEN, T. & HELAL, A. 2006. *Reductive leaching of manganese from low grade Sinai ore in HCl using H2O2 as reductant.* Hydrometallurgy, 84**,** 187-191.

FEGADE, S. L., TANDE, B. M., CHO, H., SEAMES, W. S., SAKODYNSKAYA, I., MUGGLI, D. S. & KOZLIAK, E. I. 2013. *Aromatization of propylene over Hzsm-5: A design of experiments (DOE) approach.* Chemical Engineering Communications, 200**,** 1039-1056.

GADD, G. M. 1999. *Fungal production of citric and oxalic acid: importance in metal speciation, physiology and biogeochemical processes.* Advances in microbial physiology. Elsevier.

GODUNOV, E., ARTAMONOVA, I., GORICHEV, I. & LAINER, Y. A. 2012. *Influence of oxalic acid on the dissolution kinetics of manganese oxide.* Russian metallurgy (Metally), 2012**,** 935-941.

HABASHI, F. 1993. *A textbook of hydrometallurgy, metallurgie extractive* Quebec. Enr. Que., Canada.

HARIPRASAD, D., DASH, B., GHOSH, M. & ANAND, S. 2007. *Leaching of manganese ores using sawdust as a reductant.* Minerals Engineering, 20**,** 1293-1295.

HARIPRASAD, D., MOHAPATRA, M. & ANAND, S. 2018. *Reductive Leaching of Manganese Nodule Using Saw Dust in Sulphuric Acid Medium.* Transactions of the Indian Institute of Metals, 71**,** 2971-2983.

HOSEINIAN, F., REZAI, B. & KOWSARI, E. 2019. *Optimization and separation mechanism of Ni (II) removal from synthetic wastewater using response surface method.* International Journal of Environmental Science and Technology, 16**,** 4915-4924.

KHAN, M. H. & KURNY, A. 2014. *Kinetics of simultaneous dissolution of zinc and manganese from electrolyte paste of spent zinc-carbon dry cell battery in sulfuric acid solution.* Materials Science and Metallurgy Engineering, 2**,** 1-4.

KUSUMANINGRUM, R., FITROTUROKHMAH, A., SINAGA, G., WISMOGROHO, A., WIDAYATNO, W., DIGUNA, L. & AMAL, M. *Study: leaching of zinc dust from electric arc furnace waste using oxalic acid. IOP Conference Series: Materials Science and Engineering,* 2019. IOP Publishing, 012015.

MEHDILO, A., IRANNAJAD, M. & HOJJATI-RAD, M. R. 2013. *Characterization and beneficiation of iranian low-grade manganese ore.* Physicochemical Problems of Mineral Processing, 49.

MYERS, R. H., MONTGOMERY, D. C. & ANDERSON-COOK, C. M. 2016. *Response surface methodology: process and product optimization using designed experiments*, John Wiley & Sons.

PAGNANELLI, F., FURLANI, G., VALENTINI, P., VEGLIÒ, F. & TORO, L. 2004. *Leaching of low-grade manganese ores by using nitric acid and glucose: optimization of the operating conditions.* Hydrometallurgy, 75**,** 157-167.

QING, T., ZHONG, H., SHUAI, W., LI, J.-Z. & LIU, G.-Y. 2014. *Reductive leaching of manganese oxide ores using waste tea as reductant in sulfuric acid solution.* Transactions of Nonferrous Metals Society of China, 24**,** 861-867.

SAHOO, R., NAIK, P. & DAS, S. 2001. *Leaching of manganese from low-grade manganese ore using oxalic acid as reductant in sulphuric acid solution.* Hydrometallurgy, 62**,** 157-163.

SHENG, Y. & QIU, Y.-R. 2014. *Preparation of electronic grade manganese sulfate from leaching solution of ferromanganese slag.* Transactions of Nonferrous Metals Society of China, 24, 3716-3721.

SOBOUTI, A., REZAI, B., HOSEINIAN, F. S. & MORADKHANI, D. 2019. *Optimization and kinetics studies of lead concentrate leaching using fluoroboric acid.* Physicochemical Problems of Mineral Processing, 55.

SUN, W.-Y., SU, S.-J., WANG, Q.-Y. & DING, S.-L. 2013. *Lab-scale circulation process of electrolytic manganese production with low-grade pyrolusite leaching by SO2.* Hydrometallurgy, 133**,** 118-125.

VU, H., JANDOVA, J., LISA, K. & VRANKA, F. 2005. *Leaching of manganese deep ocean nodules in FeSO4–H2SO4–H2O solutions.* Hydrometallurgy, 77, 147-153.

WANG, Y., JIN, S., LV, Y., ZHANG, Y. & SU, H. 2017. *Hydrometallurgical process and kinetics of leaching manganese from semi-oxidized manganese ores with sucrose.* Minerals, 7, 27.

WU, F.-F., ZHONG, H., WANG, S. & LAI, S.-F. 2014. *Kinetics of reductive leaching of manganese oxide ore using cellulose as reductant.* Journal of Central South University, 21, 1763-1770.

ZHANG, C., WANG, S., CAO, Z.-F. & ZHONG, H. 2018a. *Kinetics and mechanism of one-step reductive leaching of manganese oxide ores by EDTA/EDTA-2Na.* Physicochemical Problems of Mineral Processing, 54, 858–867.

ZHANG, C., WANG, S., CAO, Z.-F. & ZHONG, H. 2018b. *Recovery of manganese from manganese oxide ores in the EDTA solution.* Metallurgical Research & Technology, 115, 306.

ZHANG, W. & CHENG, C. Y. 2007. *Manganese metallurgy review. Part I: Leaching of ores/secondary materials and recovery of electrolytic/chemical manganese dioxide.* Hydrometallurgy, 89, 137-159.

ZHANG, Y., YOU, Z., LI, G. & JIANG, T. 2013. *Manganese extraction by sulfur-based reduction roasting–acid leaching from low-grade manganese oxide ores.* Hydrometallurgy, 133, 126-132.